Received: 21 March 2021 | Accepted: 22 April 2021

DOI: 10.1002/bio.4063

RESEARCH ARTICLE

LUMINESCENCE The Journal of Biological and Chemical Luminescence WILEY

Benzimidazole-based turn-on fluorescence probe developed for highly specific and ultrasensitive detection of hypochlorite ions in living cells

Yi Yang[1,2] | Siyao Cheng[2] | Wei Dong[2]

[1]Outpatient Department, First Affiliated Hospital of Nanjing Medical University, Nanjing, China

[2]School of Chemical Engineering, Nanjing University of Science and Technology, Nanjing, China

Correspondence
Wei Dong, School of Chemical Engineering, Nanjing University of Science and Technology, Nanjing, 210094, China.
Email: weidong@njust.edu.cn

Funding information
National Natural Science Foundation of China (NSFC), Grant/Award Number: 51573078

Abstract

Hypochlorite (ClO^-), as one of the active oxygen species (ROS), plays an essential role in the cellular defence system and organism immunity. In this paper, we successfully synthesized a new 'turn-on' fluorescent probe **BMF** based on benzimidazole and characterized it by spectroscopic methods. The designed probe can quickly respond to ClO^- with the obvious colour change from pink to colourless. Notably, the probe **BMF** exhibited almost no fluorescence, but showed strong fluorescence after adding ClO^-, including an excellent fluorescence turn-on effect. The fluorescence turn-on phenomenon of **BMF** was attributed to the strong oxidation of ClO^-, which severed the connecting double bond and disrupted the intramolecular charge transfer (ICT) system, plus light-induced electron transfer effect between the fluorophore and the recognition group was discontinued. In addition, the cytotoxicity assay showed that the probe had lower cytotoxicity. Based on these advantages, we demonstrated that probe **BMF** might be a good candidate for detecting ClO^- in biological systems.

KEYWORDS
benzimidazole, cell imaging, fluorescent probes, ICT change

1 | INTRODUCTION

Reactive oxygen species (ROS) are significant substances in the human body, and mainly include hydroxide ions (OH^-), oxygen (O_2), hydrogen dioxide (H_2O_2), nitrite (NO_2^-), and hypochlorite (ClO^-). Hypochlorite (ClO^-), as active oxygen species, also plays an important role in functioning of the human body as it is produced biologically in organisms by the catalysis of chloride ions (Cl^-) and H_2O_2 through the enzyme myeloperoxidase.[1,2] ClO^- plays an essential role in various physiological and pathological processes, including preventing infection and destroying pathogens.[3–5] Therefore, abnormal ClO^- concentration levels can lead to oxidative stress, tissue lesion, and many relative risks related to immune deficiency, myocardial injury, nerve damage, kidney disease, cardiovascular disease, and tumours.[6–11] Therefore, designing and developing efficient, as well as convenient, monitoring methods that can detect ClO^- is significant.

To date, various monitoring methods have been successfully applied to the determination of ClO^-, including potentiometric, electrochemical, chemiluminescence, and fluorescence analyses and methods.[12–16] Fluorescence imaging technology is considered a promising method for monitoring biological species in living cells due to its incomparable advantages of efficiency, simple processing, and high spatial and temporal resolution.[17–28] A highly fluorescent product is produced by the specific reaction between the identifying group and HClO/ClO^-, which is the design strategy of the HClO/ClO^- fluorescent probe.[29–31] Although some fluorescent probes of ClO^- already exist, some of these have disadvantages of long, time-consuming methodology, high detection limits, and the inability to be detected in living cells, which limits their application in detection of ClO^-.[32–37] In addition, some probes show the typical 'turn off' feature, which makes visual detection of ClO^- inconvenient.[38] Therefore, the development of 'turn-on' fluorescent probes is of great significance in the field of bioimaging.

Here, we prepared a benzimidazole–furfural conjugate probe **BMF**, which is displayed in Scheme 1, as a turn-on fluorescent probe to detect ClO^- in dimethyl sulphoxide (DMSO)–H_2O solution (1:1, v/v). The furfural moiety is the fluorophore part, and the benzimidazole moiety is the recognition group part containing the electron donor. There is a photo-induced electron transfer effect between the fluorophore and the recognition group that inhibits the occurrence of fluorescence. The colour of the **BMF** solution was observed to change from pink to colourless under natural light, in that the intramolecular charge transfer (ICT) and photo-induced electron transfer (PET) mechanisms were interrupted due to the oxidation effect of ClO^-. Spectroscopic experiments showed that **BMF** gave an excellent performance for selective and sensitive detection of ClO^- in DMSO–H_2O solution (1:1, v/v). In addition, the cytotoxicity assay showed that the probe had low cytotoxicity, in addition the cell imaging test showed that the probe could be used with excellent biocompatibility to detect endogenous ClO^- in L929 fibroblast cells.

2 | EXPERIMENTAL

2.1 | Chemicals

All reagents and solvents used in this work were purchased from commercial suppliers and used without further purification. 4-Nitroaniline, sodium nitrite, and furfural were purchased from Sinopharm Chemical Reagent Co., Ltd, Shanghai, China, or Nanjing Chemical Reagent Co., Ltd, Nanjing, China.

2.2 | Apparatus

Fluorescence spectra from our samples were measured using a Shimadzu RF-5301 fluorescence spectrophotometer. pH values for our samples were measured using a Sartorius (PB-10) digital pH meter (LeiCi, Shanghai, China). The morphology of the samples was investigated using scanning electron microscopy (NanoSEM 450 microscope). ^{1}H NMR spectra were characterized on a Mercury-400BB spectrometer. Cell viability was determined using the Thermo Scientific Multiskan MK3 spectrophotometer. Cell images were taken with a confocal fluorescence microscope.

2.3 | Synthesis of probe BMF

Synthesis steps were as follows. *p*-Nitroaniline (4.1 g), hydrochloric acid (8 ml) and water (16 ml) were added into a round-bottomed flask and heated, then the solution was stirred to precipitate crystals under ice bath conditions. Sodium nitrite (6 g) in water (9 ml) was added dropwise into a hydrochloric acid solution of *p*-nitroaniline and left to react for 30 min after addition. Furaldehyde (2.9 g), acetone (20 ml) and water (40 ml) were added to the filtrate, which was stirred in an ice-water bath. Copper chloride (0.8 g) was dissolved in a small amount of water, then the copper chloride solution was dripped into the filtrate and stirring continuously at room temperature for 8 h. After the reaction finished, a brick-red precipitate was formed, filtered using suction, and recrystallized with dimethyl formamide (DMF) to obtain the 5-(4-nitrophenyl)-2-furaldehyde (desired product). The 5-(4-nitrophenyl)-2-furaldehyde (1 mmol) and 2-acetonitrile benzothiazole (1 mmol) were added to the ethanol solution with triethylamine as a catalyst. The reaction was carried out for 5 h and thin-layer chromatography was used to monitor the reaction product. When the reaction was completed, the product was solidified from the reaction mixture and purified using column chromatography to get a red solid powder (**BMF**).

2.4 | General procedures for spectroscopic tests

All spectroscopic tests are carried out in DMSO/PBS solution (1:1, v/v). Stock solutions for other analyses (Cys, Tyr, Arg, Gly, Met, Phe, Leu, Lys, Thr, Try, Val, Glu, Asp, Pro, Hyd, Ser, Al^{3+}, Ca^{2+}, Cu^{2+}, Fe^{2+}, Ni^{2+}, Mg^{2+}, Na^+, K^+, NH_4^+, F^-, Cl^-, Br^-, I^-, AcO^-, SO_4^{2-}, CO_3^{2-}, NO_3^-, NO, $ONOO^-$, H_2O_2, $^{\bullet}OH$ and ClO^-) were prepared at 50 mM using deionized water. The fluorescence spectra were recorded using a fluorescence spectrometer.

2.5 | Cytotoxicity assay

The methyl thiazolyl tetrazolium (MTT; 10 μM) assay was used to measure the cytotoxicity of **BMF** with L929 cells.[39] Here, 96-well plates were used to seed L929 cells at a density of 7×10^3 cells per well and cells were incubated for 24 h at 37°C in a 5% CO_2 in air

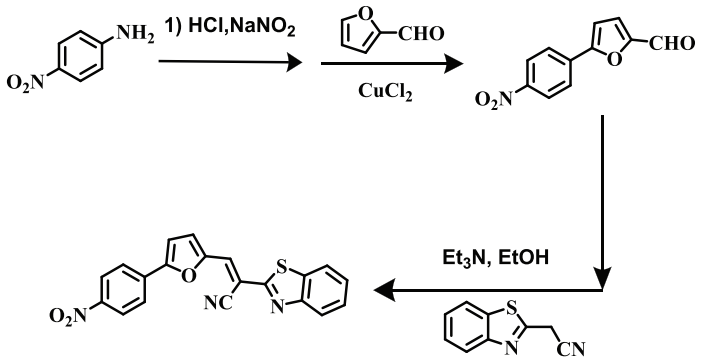

SCHEME 1 Synthesis of probe **BMF**

incubator. Specified concentrations of probes **BMF** (0, 0.01, 0.1, 1.0, 5.0 and 10 μM) were then added to the cells and all experiments for different concentrations were repeated three times. The above cells were cultured under identical conditions, and MTT solution was added within the same hour. Then, PBS buffer was incorporated into each well to eliminate unreacted MTT and the resulting formazan crystal in L929 cells was dissolved using DMSO. Absorbance at 545 nm was recorded using a Thermo Scientific Multiskan MK3 spectrophotometer.

2.6 | Cell culture and imaging

L929 cells were incubated in Dulbecco's modified Eagle's medium supplemented with 10% fetal bovine serum, 100 μg/ml penicillin and 100 μg/ml streptomycin at 37°C in a 5% CO_2 in air incubator.[40] Then 24-well plates were used to seed L929 cells for 24 h to obtain a monolayer of cells. The prepared probe **BMF** (5 μM) was put into wells to incubate for 1 h, followed by the addition of NaClO solution (0, 5 and 10 μM). Then, the combination process between probe and ClO^- was conducted for 30 min. The results of tests were photographed using the red channel (λ_{em} = 570–620 nm) of a confocal fluorescence microscopy.

3 | RESULTS AND DISCUSSION

3.1 | Designment and preparation of fluorescence probe BMF

The method for synthesizing probe **BMF** through the aldol condensation mechanism is sketched out in Scheme 1. First of all, a diazotization reaction was used to make the 4-nitroaniline generate diazonium salt, which was then reacted with furan-2-carbaldehyde using the Sandmeyer synthesis method to generate the furfural derivative part. Then, the furfural derivative part was reacted with 2-(benzothiazol-2-yl)acetonitrile to generate probe **BMF**, which is connected by a vinyl group. The linkage C=C moiety could enable the conjugated structure of molecule to be more extended and the capability for electron transfer stronger. The furfural moiety is the fluorophore part, while the benzimidazole moiety is the recognition group part containing the electron donor. There was a PET effect between the fluorophore and the recognition group, which inhibited the occurrence of the fluorescence. The structural conformation of **BMF** was identified using ^{1}H NMR and mass spectrometry (MS) at high resolution.

3.2 | Optimization conditions of ClO^- probing for probe BMF

The pH of the environment where a probe is located is an important factor that affects a probe's sensitivity and selectivity for detecting ClO^-.[41,42] Figure 1a shows the effects of acid solutions on the fluorescence intensity of **BMF** and **BMF–ClO$^-$**. The fluorescence intensity of **BMF** was stable at pH 3.0–9.0, while the fluorescence intensity of **BMF–ClO$^-$** did not show any obvious change at pH 3.0–11.0. It was indicated that the acidity of the solution had little effect on the detection of ClO^-. Therefore, pH 7.1 (common use) was selected as the optimized condition for further experiments. Based on the optimized condition, colour changes of probe **BMF** for monitoring ClO^- were observed in the DMSO/PBS buffer (v/v, 1:1, pH 7.1). From Figure 1b, it was seen that, after addition of ClO^-, the colour of **BMF** solution changed from pink to colourless under natural light and changed from pink to bright blue fluorescence under an ultraviolet (UV) light lamp with 365 nm wavelength.

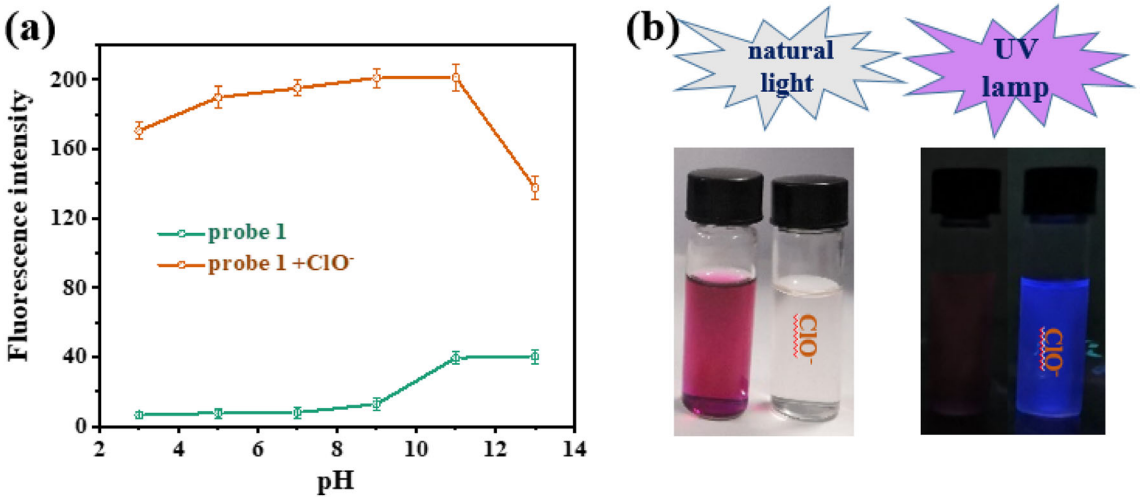

FIGURE 1 (a) Fluorescence intensity of probe **BMF** and probe **BMF** with ClO^- at 513 nm by pH values according to fluorescence titration (pH 3.0–13.0). (b) Colour changes of probe **BMF** after adding ClO^- under natural light or UV lamp

3.3 | Specificity and selectivity of probe BMF for detecting ClO^-

To study the ability of probe **BMF** to specifically recognize anions, we conducted experiments using a fluorescence spectrometer and results are shown in Figure 2a. In the fluorescence spectrum, fluorescence intensity at 513 nm did not demonstrate any obvious change in the presence of other species including Cys, Tyr, Arg, Gly, Met, Phe, Leu, Lys, Thr, Try, Val, Glu, Asp, Pro, Hyd, Ser, Al^{3+}, Ca^{2+}, Cu^{2+}, Fe^{2+}, Ni^{2+}, Mg^{2+}, Na^+, K^+, NH_4^+, F^-, Cl^-, Br^-, I^-, AcO^-, SO_4^{2-}, CO_3^{2-}, NO_3^-, NO, $ONOO^-$, H_2O_2, or $^{\bullet}OH$ at 0.5 nM concentration, except for ClO^-. As is shown in Figure 2b, there were no observable changes in fluorescence intensity with respect to the coexistence of ClO^- and other substances through various contrast experiments. This indicated that **BMF** had excellent anti-interference capacity for ClO^- following the addition of other common competing ions and that **BMF** was stable over a certain pH range, so that it could be applied in biological cells for detecting ClO^-.

3.4 | Sensing mechanism and binding behaviour of probe with ClO^-

The reaction mechanism between **BMF** and ClO^- was investigated through ^1H NMR titration experiments and MS methods. Probe **BMF** and sodium hypochlorite were added to DMSO-d6 solution separately, and then sodium hypochlorite solution was added dropwise to the **BMF** solution. As shown in Figure 3b, in the presence of ClO^-, the original proton signals of ethylene at 7.63 ppm gradually decreased to extinction and a new aldehyde proton signals at 9.62 ppm appeared at the same time, indicating that the ClO^- had oxidized and broken the ethylene double bond. As the ethylene double bond was broken, the original conjugated system of probe was destroyed and the original proton signals from probe **BMF** moved upfield dramatically. The reaction mechanism of **BMF** and ClO^- was verified by MS spectra (Figure 4), in which two peaks at 176.08 m/z and 217.04 m/z were seen. SEM images of the **BMF** powder are shown in Figure 5. Figure 5a,b demonstrates the stick-like structure with clear shape boundaries and relatively smooth surfaces; the stick-shaped powder structures were *c.* 5 μm in diameter and 50 μm in length. After ClO^- addition (Figure 5c,d) the powder became needle-like with a length of *c.* 10 μm, and seemed to aggregate into clusters. These results demonstrated that the probe reaction with ClO^- would lead to changes in the conjugation structure of the probe and produce the main fluorophore 5-(4-nitrophenyl)-2-furaldehyde.

The Gaussian 09 program at the B3LYP/6–31 G(d) level was used to complete the binding mechanism of **BMF** and the oxidant. Density-functional theory optimal configurations for **BMF** and **BMF–ClO**$^-$ are shown in Figure 6. The highest occupied orbit of **BMF** was uniformly distributed on the furfural moiety and the

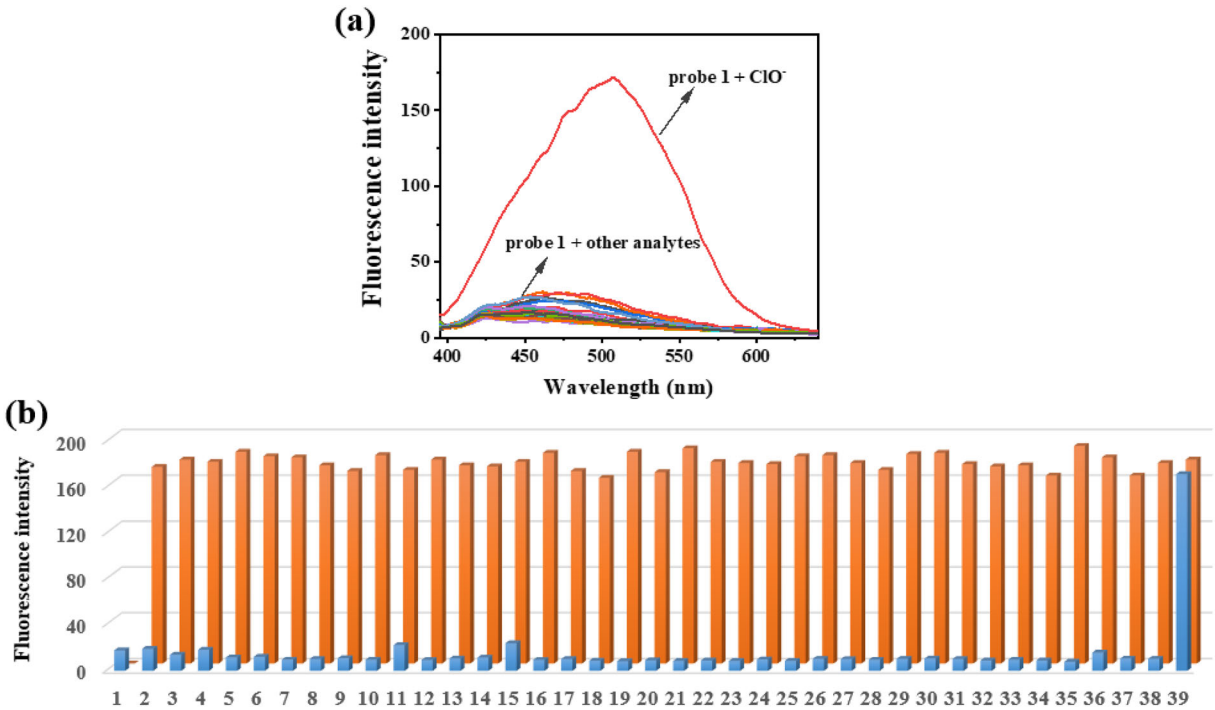

FIGURE 2 (a) Fluorescence response of probe **BMF** with various analytes in DMSO/PBS buffer (1:1, v/v). (b) Fluorescence intensity of **BMF** with ClO^- at 513 nm in the presence of other substances at 0.5 nM (1, none; 2, Cys; 3, Tyr; 4, Arg; 5, Gly; 6, Met; 7, Phe; 8, Leu; 9, Lys; 10, Thr; 11, Try; 12, Val; 13, Glu; 14, Asp; 15, Pro; 16, Hyd; 17, Ser; 18, Al^{3+}; 19, Ca^{2+}; 20, Cu^{2+}; 21, Fe^{2+}; 22, Ni^{2+}; 23, Mg^{2+}; 24, Na^+; 25, K^+; 26, NH_4^+; 27, F^-; 28, Cl^-; 29, Br^-; 30, I^-; 31, AcO^-; 32, SO_4^{2-}; 33, CO_3^{2-}; 34, NO_3^-; 35, NO; 36, $ONOO^-$; 37, H_2O_2; 38, $^{\bullet}OH$; and 39, ClO^-) in DMSO/PBS (1:1, v/v). Data were obtained 30 min after addition of the analyte. $\lambda_{ex} = 469$ nm. Slit widths: $W_{ex} = 5$ nm, $W_{em} = 10$ nm

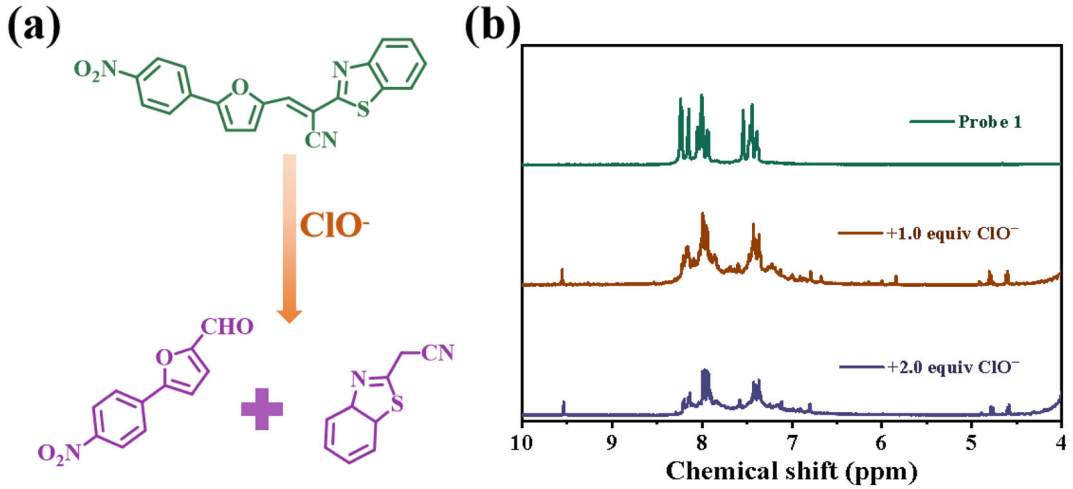

FIGURE 3 (a) Oxidation reaction of **BMF** solution with added ClO^- solution. (b) ^1H NMR spectra of probe **BMF** in DMSO-d6 without ClO^- and with presence of 1.0 equiv and 2.0 equiv ClO^- respectively

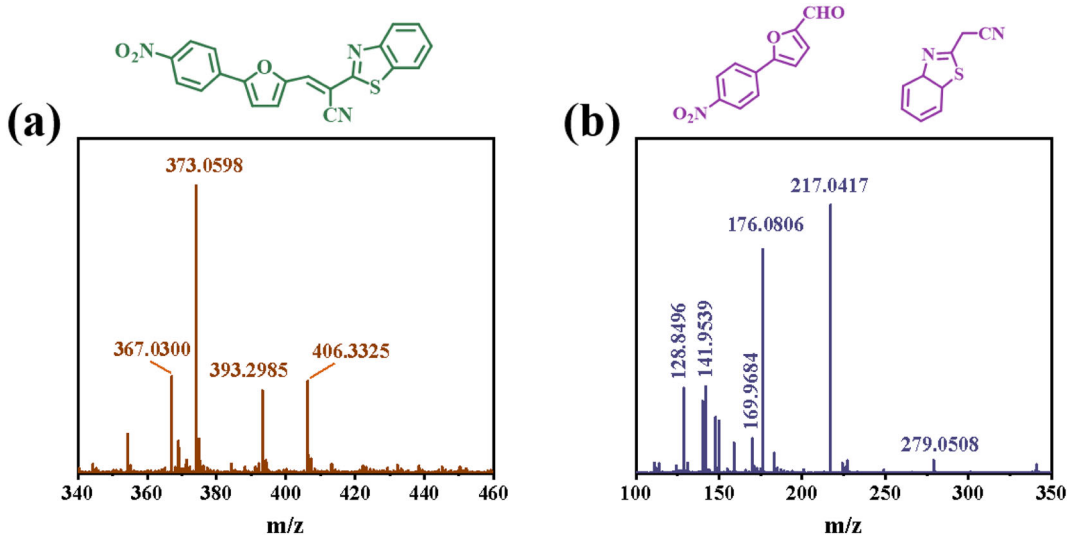

FIGURE 4 (a) MS of probe **BMF** in DMSO-d6 without the presence of ClO^-. (b) MS of probe **BMF** in DMSO-d6 with the presence of ClO^-

benzothiazole moiety because of integral π-conjugation and vibrant ICT effect. With the existence of ClO^-, the π-conjugate state of **BMF** was broken in that the C=C bond was oxidized by ClO^- and ICT process was interrupted, which indicated that the electronic cloud of **BMF–ClO⁻** was located in the furfural moiety and benzothiazole moiety. In addition, **BMF** decomposed into furfural and benzothiazole derivative during the reaction. The band gap for the furfural part (5.411 eV) notably exceeded the band gap for **BMF** (2.853 eV), which demonstrated that the furfural part could make probe **BMF** specific for ClO^-, and the band gap of the benzothiazole part also exceeded the band gap for **BMF**. Therefore, we could conclude that **BMF** detected ClO^- through a nucleophilic addition reaction and then decomposition.

3.5 | Biocompatibility and bioimaging features in L929 cells

To extend the utility value of the probe **BMF** in the field of biology, biocompatibility of the probe was tested in L929 cells.[43,44] Standard MTT assay is an essential assessment criteria to investigate potential toxicity. As shown in Figure 7, the survival rate of cells exceeded 80%, even if the concentration of probe **BMF** reached 10 μM. Therefore, probe **BMF** demonstrated the potential for application for probing ClO^- in living cells. As shown in Figure 8, probe **BMF** could enter cells and diffuse throughout the cytoplasm. After incubating cells for 30 min at 37°C in the presence of **BMF** (5 μM), they displayed a completely black colour with no red fluorescence. As the

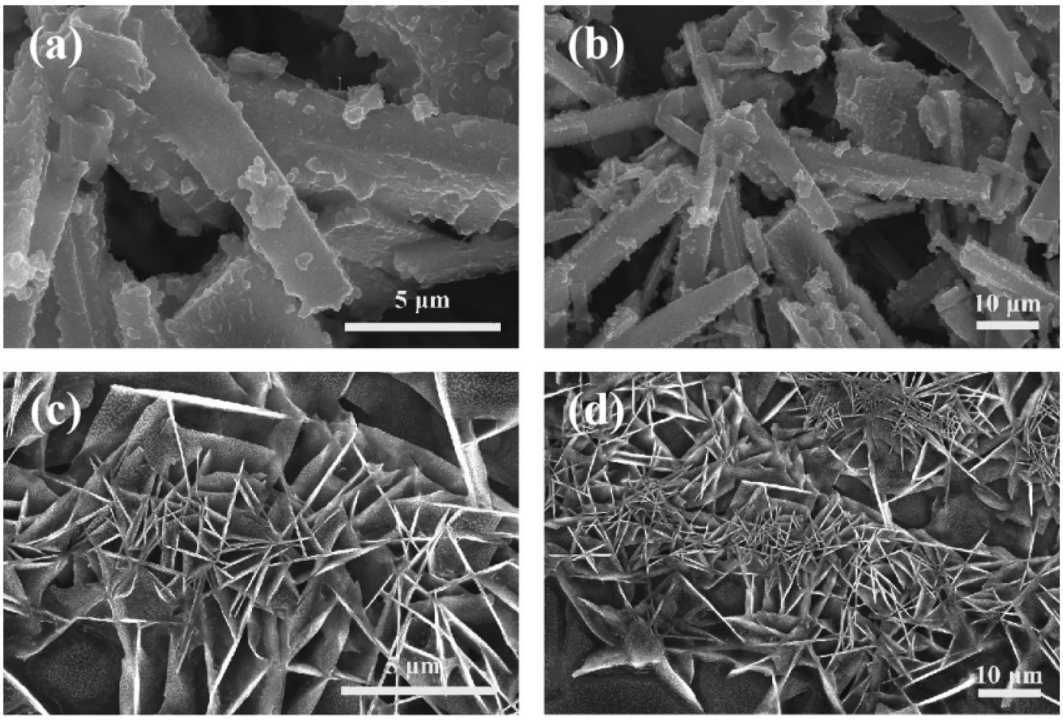

FIGURE 5 Scanning electron microscope (SEM) images of the **BMF** powder and **BMF–ClO⁻** powder. (a) **BMF** (5 μm); (b) **BMF** (10 μm); (c) **BMF–ClO⁻** (5 μm); and (d) **BMF–ClO⁻** (10 μm)

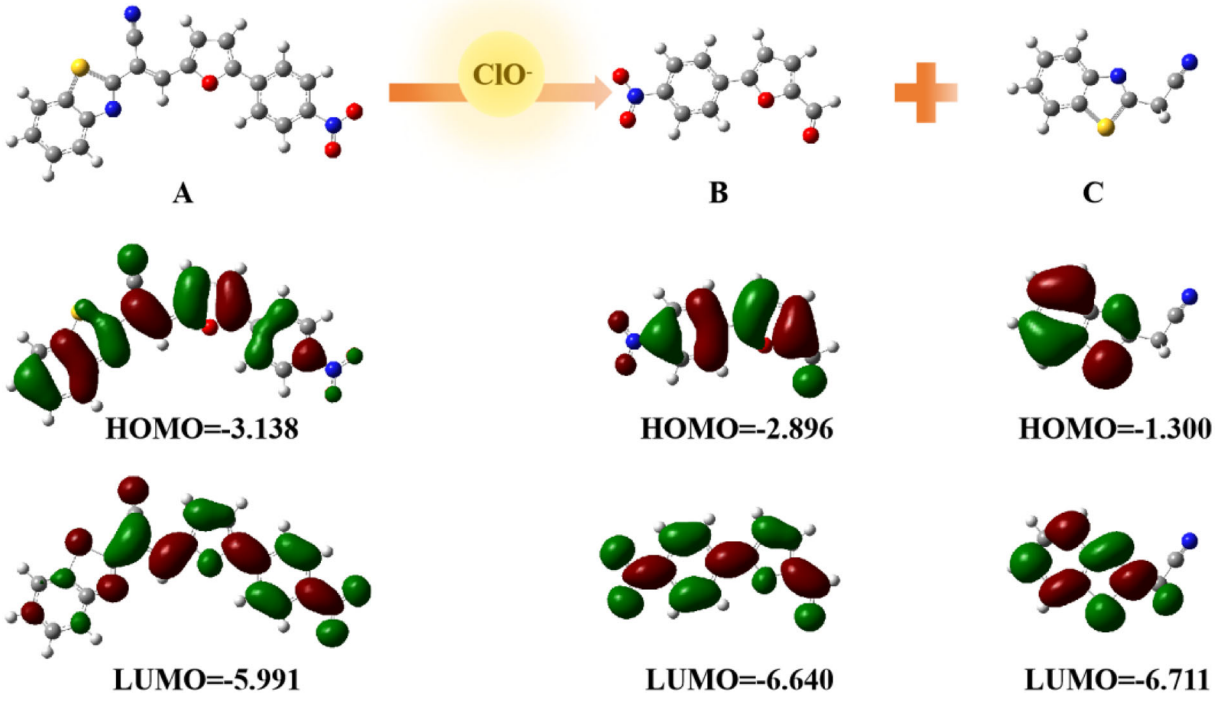

FIGURE 6 Energy diagrams of optimized configurations, the highest and lowest occupied orbits of **BMF** and decomposition products of **BMF–ClO⁻**. A, **BMF**; B, furfural derivative; C, benzothiazole derivative

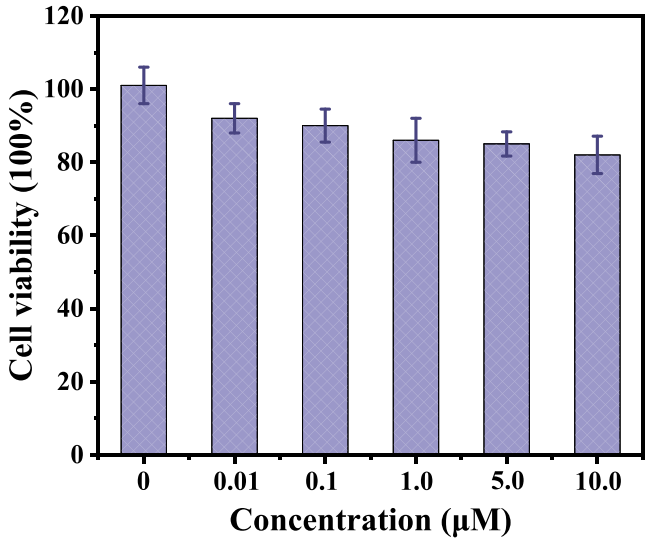

FIGURE 7 Cell cytotoxicity assay of different concentrations of probe **BMF** solution in L929 cells. 0 μM, contrast

concentration of ClO^- increased, red fluorescence from the L929 cells began to appear and became stronger and stronger until strong red fluorescence was produced. These results demonstrated that probe **BMF** had good cell permeability and could be used for ClO^- detection in biological cells.

4 | CONCLUSION

In summary, we have successfully prepared a 'turn-on' fluorescent probe **BMF**. Probe **BMF** displayed high selectivity for ClO^- rather than other ROS and analytes because of the presence of a unique recognition unit of an ethylene double bond group. In addition, the probe solution could quickly respond to ClO^- with an obvious colour change from pink to colourless under natural light. Notably, probe **BMF** produced almost no fluorescence, but exhibited a strong fluorescence enhancement at 513 nm after addition of ClO^-, showing an excellent fluorescence turn-on effect. Furthermore, cytotoxicity tests and

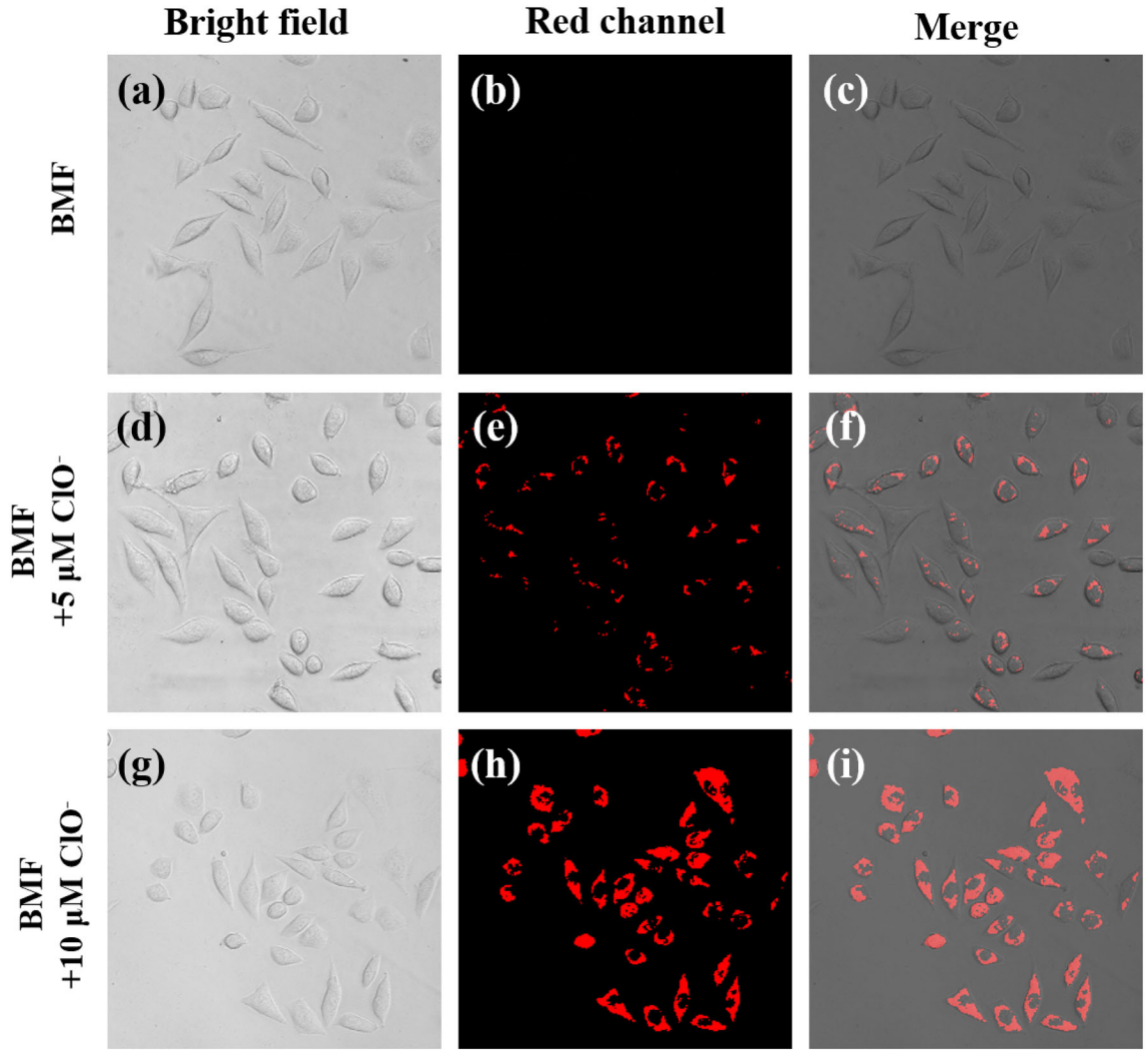

FIGURE 8 Confocal fluorescence microscopy photographs of NaClO detection in L929 cells with probe **BMF**. L929 cells treated with 5 μM **BMF** (a–c), then further incubated with 5 μM ClO^- (d–f) and 10 μM ClO^- (g–i). Fluorescence images from left to right: red channel and merged images (red channel, λ_{em} = 580–630 nm)

bioimaging experiments showed that **BMF** had excellent biocompatibility and cytomembrane-permeable capacity. To sum up, probe **BMF** has a broad prospect of application for realistic detection of ClO^- in living organisms due to the above results.

ACKNOWLEDGEMENTS

We acknowledge the financial support by the National Natural Science Foundation of China (NSFC) (grant number 51573078).

CONFLICT OF INTEREST

The authors have declared no conflict of interest.

ORCID

Wei Dong https://orcid.org/0000-0002-6712-8960

REFERENCES

[1] D. Roos, C. C. Winterbourn, *Science* **2002**, *296*, 669.
[2] C. C. Winterbourn, M. B. Hampton, J. H. Livesey, A. J. Kettle, *J. Biol. Chem.* **2006**, *281*, 39860.
[3] D. I. Pattison, M. J. Davies, *Biochemistry* **2006**, *45*, 8152.
[4] M. Maden, I. F. Ertugrul, E. O. Orhan, C. E. Erik, C. C. Yetis, Y. Tuncer, M. Kahriman, *PLoS One* **2017**, *12*, 183895.
[5] J. E. Harrison, J. Schultz, *J. Biol. Chem.* **1976**, *251*, 1371.
[6] S. Khatib, R. Musa, J. Vaya, *Bioorg. Med. Chem.* **2007**, *15*, 3661.
[7] Y. W. Yap, M. Whiteman, N. S. Cheung, *Cell. Signal.* **2007**, *19*, 219.
[8] C. H. Sam, H. K. Lu, *J. Dent. Sci.* **2009**, *4*, 45.
[9] Y. Maruyama, B. Lindholm, P. Stenvinkel, *J. Nephrol.* **2004**, *17*, 72.
[10] E. Malle, T. Buch, H. J. Grone, *Kidney Int.* **2003**, *64*, 1956.
[11] M. J. Steinbeck, L. J. Nesti, P. F. Sharkey, J. Parvizi, *J. Orthop. Res.* **2007**, *25*, 1128.
[12] L. C. Adam, G. Gordon, *Anal. Chem.* **1995**, *67*, 535.
[13] S. Thiagarajan, Z. Y. Wu, S. M. Chen, *J. Electroanal. Chem.* **2011**, *661*, 322.
[14] L. L. Shi, X. Li, M. Zhou, F. Muhammad, Y. B. Ding, H. Wei, *Analyst* **2017**, *142*, 2104.
[15] D. F. Marino, J. D. Ingle, *Anal. Chem.* **1981**, *53*, 455.
[16] L. Q. Yan, C. J. Hu, J. P. Li, *Anal. Bioanal. Chem.* **2018**, *410*, 7457.
[17] H. Zhu, J. Fan, B. Wang, X. Peng, *Chem. Soc. Rev.* **2015**, *44*, 4337.
[18] J. Fan, M. Hu, P. Zhan, X. Peng, *Chem. Soc. Rev.* **2013**, *42*, 29.
[19] Z. Xu, J. Yoon, D. R. Spring, *Chem. Soc. Rev.* **2010**, *39*, 1996.
[20] J. Du, M. Hu, J. Fan, X. Peng, *Chem. Soc. Rev.* **2012**, *41*, 4511.
[21] Q. Xu, P. Pu, J. Zhao, C. Dong, C. Gao, Y. Chen, J. Chen, Y. Liu, H. Zhou, *J. Mater. Chem. A* **2015**, *3*, 542.
[22] K. Huang, C. Jiang, A. A. Martí, *J. Phys. Chem. A* **2014**, *118*, 10353.
[23] L. Zhu, Z. Yuan, J. T. Simmons, K. Sreenath, *RSC Adv.* **2014**, *4*, 20398.
[24] Z. Yu, R. M. Schmaltz, T. C. Bozeman, R. Paul, M. J. Rishel, K. S. Tsosie, S. M. Hecht, *J. Am. Chem. Soc.* **2013**, *135*, 2883.
[25] Z. Yu, T. Kabashima, C. Tang, T. Shibata, K. Kitazato, N. Kobayashi, M. K. Lee, M. Kai, *Anal. Biochem.* **2010**, *397*, 197.
[26] T. Kabashima, Z. Yu, C. Tang, Y. Nakagawa, K. Okumura, T. Shibata, J. Lu, M. Kai, *Peptides* **2008**, *29*, 356.
[27] J. Hu, C. J. Easley, *Analyst* **2011**, *136*, 3461.
[28] K. Sreenath, Z. Yuan, J. R. Allen, M. W. Davidson, L. Zhu, *Chem. – Eur. J.* **2015**, *21*, 867.
[29] X. Chen, X. Tian, I. Shin, J. Yoon, *Chem. Soc. Rev.* **2011**, *40*, 4783.
[30] X. Chen, X. Wang, S. Wang, W. Shi, K. Wang, H. Ma, *Chem. – Eur. J.* **2008**, *14*, 4719.
[31] P. Panizzi, M. Nahrendorf, M. Wildgruber, P. Waterman, J.-L. Figueiredo, E. Aikawa, J. McCarthy, R. Weissleder, S. A. Hilderbrand, *J. Am. Chem. Soc.* **2009**, *131*, 15739.
[32] X. Huang, Z. P. Li, T. T. Cao, Q. Cai, C. C. Zeng, H. Fu, L. Hu, *RSC Adv.* **2018**, *8*, 14603.
[33] R. X. Ji, K. Qin, A. K. Liu, Y. Zhu, Y. Q. Ge, *Tetrahedron Lett.* **2018**, *59*, 2372.
[34] Y. Q. Gong, B. Yu, W. Yang, X. L. Zhang, *Biosens. Bioelectron.* **2016**, *79*, 822.
[35] H. J. Tong, Y. J. Zhang, S. N. Ma, M. H. Zhang, N. Wang, R. Wang, K. Lou, W. Wang, *Chin. Chem. Lett.* **2018**, *29*, 139.
[36] X. D. Lou, Y. Zhang, J. G. Qin, Z. Li, *Sensor. Actuator. B Chem.* **2012**, *16*, 229.
[37] W. Y. Lin, L. L. Long, B. B. Chen, W. Tan, *Chem. – Eur. J.* **2009**, *15*, 2305.
[38] K. N. Wang, P. Z. Sun, X. J. Chao, D. X. Cao, Z. W. Mao, Z. Q. Liu, *RSC Adv.* **2018**, *8*, 6904.
[39] H. Lv, H. Sun, S. Wang, F. Kong, *Spectrochim. Acta A* **2018**, *196*, 160.
[40] S. Cheng, X. Pan, M. Shi, G. Zuo, T. Su, C. Zhang, J. Li, W. Dong, *Talanta* **2019**, *203*, 90.
[41] M. R. Awual, M. Khraisheh, N. H. Alharthi, M. Luqman, A. Islam, M. Rezaul Karim, M. M. Rahman, M. A. Khaleque, *Chem. Eng. J.* **2018**, *343*, 118.
[42] K. Abbas, H. Znad, M. R. Awual, *Chem. Eng. J.* **2018**, *334*, 432.
[43] K. B. Li, F. Z. Chen, Q. H. Yin, S. Zhang, W. Shi, D. M. Han, *Sens. Actuat. B Chem.* **2018**, *254*, 222.
[44] G. Liu, D. Liu, X. Han, X. Sheng, Z. Xu, S. H. Liu, L. Zeng, J. Yin, *Talanta* **2017**, *170*, 406.

How to cite this article: Y. Yang, S. Cheng, W. Dong, *Luminescence* **2021**, 1. https://doi.org/10.1002/bio.4063